Controllable Modulation of the Electronic Structure of ZnO(10$\bar{1}$0) Surface by Carboxylic Acids†

ARTICLE *in* THE JOURNAL OF PHYSICAL CHEMISTRY C · FEBRUARY 2010

Impact Factor: 4.77 · DOI: 10.1021/jp908517j

3 AUTHORS, INCLUDING:

Xiaoqing Tian
Shenzhen University
10 PUBLICATIONS **98** CITATIONS
SEE PROFILE

Weiguang Xie
Jinan University (Guangzhou, China)
54 PUBLICATIONS **342** CITATIONS
SEE PROFILE

Controllable Modulation of the Electronic Structure of ZnO(10$\bar{1}$0) Surface by Carboxylic Acids†

Xiaoqing Tian,‡,§ Jianbin Xu,*,‡ and Weiguang Xie‡

Department of Electronic Engineering and Materials Science and Technology Research Center, The Chinese University of Hong Kong, Shatin, N.T., Hong Kong SAR, People's Republic of China, and Department of Chemistry, Princeton University, New Jersey 08544

Received: September 3, 2009; Revised Manuscript Received: December 8, 2009

A systematic investigation of the correlation between bonding geometries and electronic structures of mercapto-acetic acid molecule on the ZnO(10$\bar{1}$0) nonpolar surface is reported. The geometric structure calculation results are consistent with the recent Fourier transform infrared attenuated total reflectance (FT-IR-ATR) findings. The mercapto-acetic acid molecule can contribute an abundance of band gap states to ZnO. Monolayer functionalized ZnO(10$\bar{1}$0) is on the verge of a metal to insulator transition, which is consistent with the experimental findings of the conductivity increase by 6 orders of magnitude. The electrostatic net charge transfer from the molecule to ZnO is around 0.3 electrons for all configurations, but the electronic structure and adsorption energy of carboxylic molecules on ZnO(10$\bar{1}$0) show strong configuration dependence. This is also the magic of the organic molecule-oxide interface. The mercapto-acetic acid molecule functionalized ZnO also shows facet-dependent characteristics while the monolayer functionalized ZnO(2$\bar{1}\bar{1}$0) does not show metal to insulator transition. Acetic acid does not contribute to the band gap states of ZnO(10$\bar{1}$0), whereas benzoic acid and 9-anthracenecarboxylic acid do contribute an abundance of band gap states to ZnO(10$\bar{1}$0). 9-Anthracenecarboxylic acid functionalized ZnO(10$\bar{1}$0) shows a smaller energy difference between the conduction band minimum (CBM) and highest occupied molecular orbital (HOMO), compared to mercapto-acetic acid under the same situation. Our findings are useful to understand the effect of surface functionaliztion on ZnO-based solar cells, biosensor applications, oxide surface nanofabrications, and molecular electronics.

I. Introduction

Zinc oxide has attracted a significant amount of attention in the past several years since this wide band gap semiconductor is found to have a number of potential applications in catalysis, solar cells, gas sensors, light emitting diodes (LEDs), diluted magnetic semiconductors (DMSs), and microelectronic devices. The low-index nonpolar ZnO(10$\bar{1}$0) and (2$\bar{1}\bar{1}$0) surfaces are of great interest, because they make industrial applications more favorable. Zn−O mixed (10$\bar{1}$0) and (2$\bar{1}\bar{1}$0) surfaces also appear naturally as the majority surfaces of experimentally synthesized ZnO nanoparticles, nanobelts, nanowires, and nanorods, since these nanostructures mainly grow along ⟨0001⟩ direction, and (10$\bar{1}$0) and (2$\bar{1}\bar{1}$0) appear as the major surfaces.[1] The surface energy of ZnO(10$\bar{1}$0) (2.3 J/m^2) is smaller than that of ZnO(2$\bar{1}\bar{1}$0) (2.5 J/m^2) and those of polar surfaces ZnO(0001)−Zn and ZnO(000$\bar{1}$)−O (4.0 J/m^2), which make self-compensated (10$\bar{1}$0) surface most stable.[2] M-nonpolar ZnO(10$\bar{1}$0) was also used as the substrate without template for the growth of quantum structure in which large anisotropy of conductivity was found.[3]

Functionalization of semiconductor surfaces by organic molecules is a promising route for the development of hybrid organic−inorganic devices and molecular nanostructures. The interface electronic structure between covalently attached organic layers and inorganic substrate was envisioned controllable by tuning the chemical type and composition of organic molecules.[4,5] The electronic structure of organic molecules adsorbed on surfaces has been frequently investigated by scanning tunneling microscopy and spectroscopy (STM and STS).

Dye-treated ZnO has been explored to the application of solar cells, due to its abundance of charge carriers. By use of organic molecule dye sensitized ZnO solar cell, high incident photon-to-current conversion efficiency of up to 70% were obtained.[6]

Besides photovoltaic properties of organic molecule treated ZnO, the electronic transport properties of ZnO nanostructures could also be tuned by organic molecule functionalization.[7]

Carboxylic group (−COOH) is one of the frequently used anchor groups in the biosensor and materials surface functionalization. The adsorption of −COOH on a semiconductor surface is able to enhance the electron injection into the conduction band. It has been found in recent experiments[7] that the conductivity and photoconductivity of ZnO could be enhanced by carboxylic group anchored molecule functionalization.

Here, we use the state of the art first principles technique to investigate the interactions between a series of carboxylic acid molecules and ZnO(10$\bar{1}$0) single crystalline surface. The

† Notes: All results are for ZnO(10$\bar{1}$0) except otherwise indicated. Red atoms represent oxygen atoms; ice-blue atoms represent zinc atoms; gray blue atoms represent carbon atoms; yellow atoms represent sulfur atoms; white atoms represent hydrogen atoms.

* To whom correspondence should be addressed. e-mail:jbxu@ee.cuhk.edu.hk.

‡ The Chinese University of Hong Kong.

§ Princeton University.

10.1021/jp908517j
Published on Web 02/17/2010

mercapto-acetic acid molecule, with two functional groups −COOH and −SH, is selected as the major molecule for this investigation. −COOH is normally used as the anchor for molecule's chemical bonding with semiconductor surface, while −SH is frequently used as the anchor for molecule with metal electrodes such as Au, Ag, and Cu, so that the interface between ZnO and Au can be tuned from a Schotcky contact to an Ohmic contact.[7] Besides the role of anchoring electrode, −SH itself can also affect the interfacial electronic structure between molecule and semiconductor. The coverage effects are also investigated. The interfacial electronic structures between acetic acid, benzoic acid, 9-anthracenecarboxylic acid, and ZnO($10\bar{1}0$) are calculated to check the influence of the tail and chemical composition.

II. Method

The calculations are performed within the Vienna ab initio simulation package (VASP).[8] The PW91 general gradient approximation (GGA) is used.[9,10] The electron−ion interaction is described by PAW method.[11] 29.40 Ry is used as the plane-wave basis set cutoff. The on-site coulomb interaction for Zn is used, namely, GGA+U.[12] Conventional GGA or LDA overestimates the coupling between Zn 3d and O 2p electrons. The ZnO 3d electrons also have a higher energy toward the valence band maximum (VBM) by conventional GGA or LDA. Conventional LDA or GGA treatment of ZnO has an energy gap around 0.8 eV. By DFT+U, this value can be improved, with an energy gap around 2.0 eV. However, this is still smaller than the experimental value of 3.3 eV by 39.4% but consistent with other DFT+U calculation results.[13] The Zn 3d electrons mainly locate around 3−5 eV with respect to the VBM by GGA or LDA. After introducing on-site coulomb repulsion energy U, the Zn 3d electrons can be better described and the electronic structures are consistent with XPS experiments.[14,13] The Zn 3d electrons mainly locate around 7−9 eV below valence band top.

III. Results and Discussion

Six layers of ZnO($10\bar{1}0$) 2 × 3 are used as the surface slabs for interaction of single molecule with surface, also corresponding to $^1/_6$ monolayer coverage. A 1.6-nm vacuum layer is used to eliminate the longitudinal interactions between super cells. A 5 × 5 × 1 Monkhorst-Pack *k*-point mesh is used for the surface slab calculation. A 5 × 8 × 1 Monkhorst-Pack *k*-point mesh is used for ZnO($10\bar{1}0$) 2 × 2 surface slab calculation to simulate half monolayer coverage case. The coverage is defined as the ratio of number of molecules and number of outmost surface Zn atoms. The topmost four layers of the slab and the molecule are allowed to relax until all the residual forces are lower than 20 meV/Å. The adsorption energy is calculated by the following equation

$$\Delta E = -(E - E_0 - E_{\text{adsorbate}}) \quad (1)$$

where E is the energy of ZnO($10\bar{1}0$) substrate with an adsorbate, $E_{\text{adsorbate}}$ is the energy of the molecule, and E_0 is the energy of ZnO($10\bar{1}0$) clean substrate without the adsorbate. The detailed adsorption process has been described by Newns-Anderson model.[15,16]

Five Typical Configurations with Single Molecule Adsorption. After optimization, five different configurations are considered as shown in Figure 1. Covalent adsorption of formic acid and other alkyl acids on ZnO and TiO_2 surface have been theoretically and experimentally investigated.[17−22] The adsorption energies ΔE_1 for 5 configurations are shown in Table 1. Configuration (a) and configuration (e) have the largest and second largest adsorption energies, respectively. Since each molecule in configuration (a) occupies two Zn atoms, the extreme coverage of configuration (a) is half monolayer. The coverage limit of configuration (e) is full monolayer, because each molecule occupies one Zn atom. Therefore, configuration (e) is the most stable configuration thermodynamically. Fourier transform infrared attenuated total reflectance (FT-IR-ATR) experiments on carboxylic functionalized ZnO nanotips has demonstrated the disappearance of carbonyl bond (C═O) at 1710 cm^{-1} [21], and this is consistent with our calculated most stable configuration.

The electronic coupling between adsorbed molecular orbitals and semiconductor surface can be analyzed by projected density of states (PDOS) into organic molecular orbitals and semiconductor surface.

The band gap of clean ZnO($10\bar{1}0$) is 1.22 eV, as shown in Figure 2a, and the isolated mercapto-acetic acid molecule lowest-unoccupied molecular orbital (LUMO)−HOMO gap is 4.20 eV, as shown in Figure 2b. Parts c and d of Figure 2 show the density of states (DOS) of configuration (b) and configuration (e), respectively. The ZnO surface energy gap is 1.22 eV for all configurations. The major difference is the position of HOMO of molecule. For configuration (b), the HOMO lies at 0.40 eV higher than VBM of semiconductor, and the energy difference between HOMO and CBM of semiconductor is 0.82 eV, which is about 40% smaller than the energy band gap of ZnO surface. For configuration (e), the energy difference between HOMO and CBM of semiconductor is 0.86 eV, which is about 30% smaller than the energy band gap of ZnO surface. Molecular orbitals in isolated molecule are strongly localized (Figure 2b), while adsorbed on ZnO, the molecular orbitals, such as HOMO-1 and below, have strong hybridization with ZnO valence band and tend to be more delocalized (parts c and d of Figure 2). The HOMO of molecule remains its localized characteristic.

The band gap states contributed by the organic molecule effectively facilitate decreasing the energy difference between CBM and VBM and serve as the transitional states from semiconductor's VBM to CBM. However, this conclusion remains to be further confirmed by experiments. Two channels are possible for molecule excitation from the HOMO to the LUMO of molecule, or from the HOMO directly to the CBM of semiconductor.[23]

The HOMO of dye molecules normally resides in the band gap of semiconductor, while the LUMO lies in the conduction band to gain a high efficiency of dye sensitized solar cell. So the interfacial electronic structure of mercapto-acetic acid−ZnO fulfills these two criteria. The efficiency of dye-sensitized solar cells is mainly evaluated by two factors: (1) the maximum photocurrent density, I_{ph}, corresponding to the charge injection from the HOMO of molecule into the semiconductor conduction band, and (2) the open circuit potential, V_{oc}, related to the energy difference between the HOMO and the CBM of semicondcutor.[24]

The energy difference $E^{\text{l}}_{\text{CBM-HOMO}}$ between CBM and HOMO is shown in Table 1, and it strongly depends on adsorption configurations from 0.56 to 1.10 eV. The adsorption configuration dependent electronic structure of catechol on rutile TiO_2(110) has been previously reported.[25] Electronic structure shows bonding geometry dependence and only bidendate configuration introduces band gap states into the semiconductor.

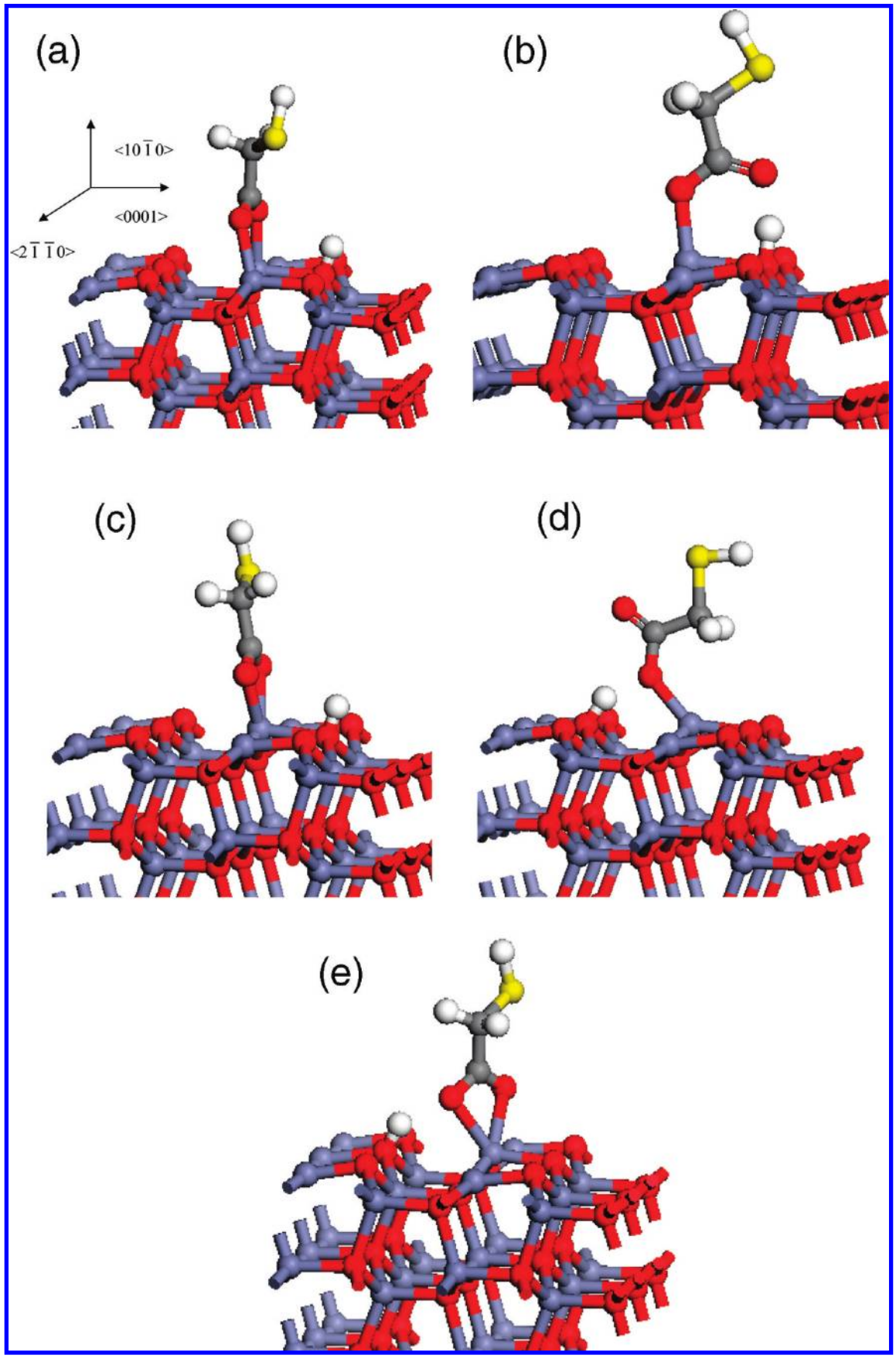

Figure 1. Five adsorption configurations of single molecule case: (a) bidentate bridging configuration, (b) monodentate ester-type configuration, (c) bidentate chelating configuration, (d) monodentate O-up configuration, (e) bidentate chelating with hydrogen bonding configuration. Oxygen atoms are red, Zinc atoms are ice-blue, Carbon atoms are gray, Sulfur atoms are yellow, and Hydrogen atoms are white. All results are for ZnO (10$\bar{1}$0) except otherwise indicated. These two notations are used throughout this paper.

TABLE 1: Adsorption Energies $\Delta E_{(1,2,3)}$ and CBM-HOMO Energy Differences $E^{(1,2,3)}_{\text{CBM-HOMO}}$ for Five Configurations at $^1/_6$, $^1/_2$, and 1 Monolayer Coverage, Respectively

	a	b	c	d	e
ΔE_1 (eV)	1.95	1.59	1.48	0.90	1.73
ΔE_2 (eV)	2.06	1.65			1.86
ΔE_3 (eV)		1.47			1.66
$E^1_{\text{CBM-HOMO}}$ (eV)	1.10	0.82	0.90	0.56	0.86
$E^2_{\text{CBM-HOMO}}$ (eV)	0.98	0.60			0.58
$E^3_{\text{CBM-HOMO}}$ (eV)		−0.35			−0.22

−COOH anchored dye on anatase TiO_2 has been studied and different adsorption modes lead to different open-circuit voltages of dye-sensitized solar cells.[26]

According to our calculations, each configuration can totally transfer around 0.3 electrons to the ZnO surface. The oxygen atom of −COOH gains electrons from surface by Zn−O bonding, while the H atom of −COOH serves as the donor to the surface by O−H bonding. The net effect between the two charge transfer pathways is that the oxide surface gains 0.3 electrons from the molecule. Generally speaking, the gained electrons from the molecule may enhance the ZnO n-type intrinsic conductivity.

The charge transfer effects are almost the same for all configurations, but electronic structures depend on specific configurations, which is also an intriguing attribute of this molecule-oxide interface.

Hydrogen adsorption on ZnO($10\bar{1}0$) surface has led to metal to insulator transition, confirmed by STS measurement.[27] Another wide bandgap SiC also shows surface metallicity after β-SiC(100) passivated by hydrogen under UHV-STM study.[28]

Coverage Dependence: Half Monolayer and Full Monolayer. For coverage dependence, bidentate bridging configuration, monodentate ester-type adsorption, and bidentate chelating with hydrogen bonding modes are mainly discussed. However, bidentate bridging configuration is lack of full monolayer coverage, since each molecule occupies two surface Zn atoms.

For half coverage, adsorption energy ΔE_2 and the CBM-HOMO energy difference $E^2_{\text{CBM-HOMO}}$ are shown in Table 1. The adsorption energies of three configurations are all higher than

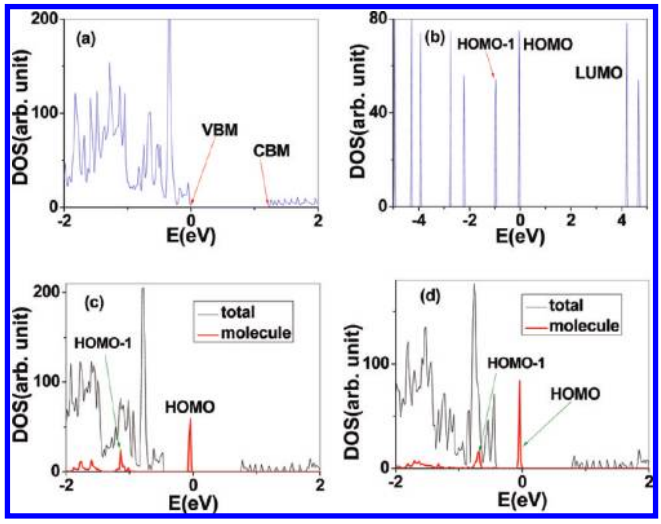

Figure 2. (a) DOS of single molecule case DOS of clean ZnO($10\bar{1}0$) with 1.22 eV band gap. (b) DOS of isolated mercapto-acetic acid molecule with 4.20 eV UMO-HOMO gap. (c) Monodentate ester-type configuration's DOS. (d) Bidentate chelating with hydrogen bonding configuration DOS.

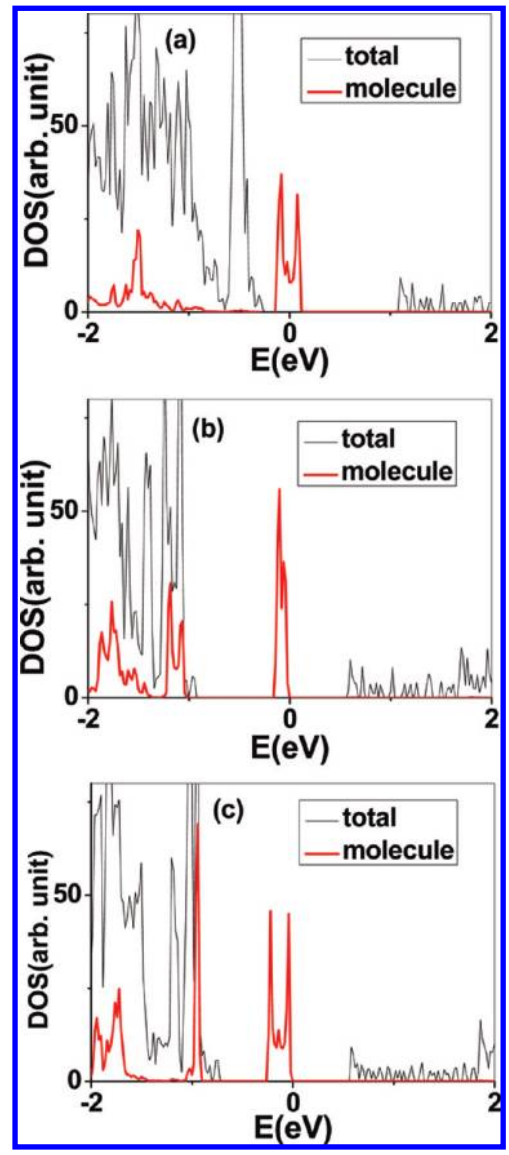

Figure 3. DOS of half monolayer coverage: (a) DOS of bidentate bridging configuration; (b) DOS of monodentate ester-type configuration; (c) DOS of bidentate chelating with Hydrogen bonding configuration.

single molecule cases due to intermolecular interactions. Actually for configurations (b) and (e), there are two growth directions for molecular assembly along $\langle 2\bar{1}\bar{1}0\rangle$ or $\langle 0001\rangle$. For configuration (b), the adsorption energy for growth along $\langle 0001\rangle$ is 0.38 eV higher than $\langle 2\bar{1}\bar{1}0\rangle$; for configuration (e), the corresponding value is 0.46 eV. So the molecules tend to assemble along $\langle 0001\rangle$ at initial growth stage, and this preferred growth direction is the same with ZnO nanostructure growth direction.

Figure 3a shows the DOS of bidentate bridging configuration, and the open circuit potential is 0.98 eV, which is about 0.12 eV less than that of $^1/_6$ monolayer coverage. Figure 3b shows the DOS of monodentate ester-type configuration, and the open circuit potential is 0.60 eV, which is about 0.15 eV less than that of $^1/_6$ monolayer coverage. Figure 3c shows the DOS of bidentate chelating with hydrogen bonding configuration, and the open circuit potential is 0.58 eV, which is about 0.28 eV less than that of $^1/_6$ monolayer coverage. The band gap states of mercapto-acetic acid with half monolayer coverage have a width around 2−3 times that of the $^1/_6$ monolayer case. The occupied molecular orbitals

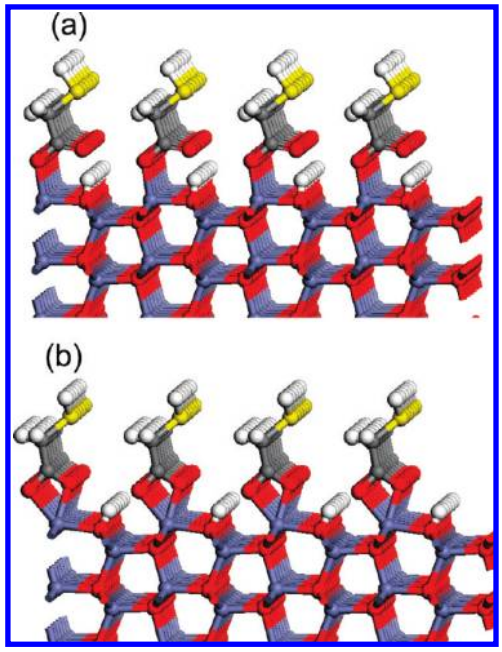

Figure 4. Structures of full monolayer coverage: (a) monodentate ester-type configuration; (b) bidentate chelating with hydrogen bonding configuration.

(below VBM) have strong hybridization with ZnO valence band and tend to be more delocalized.

For full monolayer coverage, monodentate ester-type and bidentate chelating with hydrogen bonding adsorption modes are involved. The structures after optimization are shown in parts a and b of Figure 4. Adsorption energy ΔE_3 and CBM-HOMO energy difference $E^3_{\text{CBM-HOMO}}$ are shown in Table 1. The adsorption energies are 1.47 and 1.66 eV per molecule for monodentate ester-type and bidentate chelating with hydrogen bonding configurations, respectively. The coupling between organic monolayer and semiconductor can be manifested by band structure. Figure 5a shows the band structure of monodentate ester-type configuration. The Fermi level lies around 0.35 eV higher than the CBM. The 4s orbital of Zn has been partially filled, so the semiconductor has been on the edge of metal to insulator transition. The energy gap between VBM and CBM has been filled by molecule states. The molecular monolayer contributes the continued states from 0.21 eV below the VBM to the HOMO (0.35 eV higher than CBM). The semiconductor remains its merit of direct band gap characteristic, and the energy gap is 1.22 eV. The HOMO of molecule lies at the edge of CBM. Figure 5b shows the band structure of monolayer coverage case for bidentate chelating with hydrogen bonding. The Fermi level lies around 0.22 eV higher than the CBM, so for bidentate chelating with hydrogen bonding monolayer coverage, the organic molecule-semiconductor system is also on the edge of metal to insulator transition. The molecular monolayer contributes an abundance of continuously occupied states with a width of 1.69 eV, which fully fills the band gap of ZnO. The conductive and photovoltaic performances will be pronouncedly improved. The merit of direct band gap characteristic of ZnO has also remained unchanged. These results are consistent with ref 7, which has reported experimentally that the conductance of ZnO is enhanced by 6 orders of magnitude upon mercapto-acetic acid molecule functionalization.

Facet Dependence: Monolayer Functionalized ZnO(2$\bar{1}\bar{1}$0) Surface. The interaction between mercapto-acetic acid molecule and another nonpolar majority ZnO(2$\bar{1}\bar{1}$0) surface is

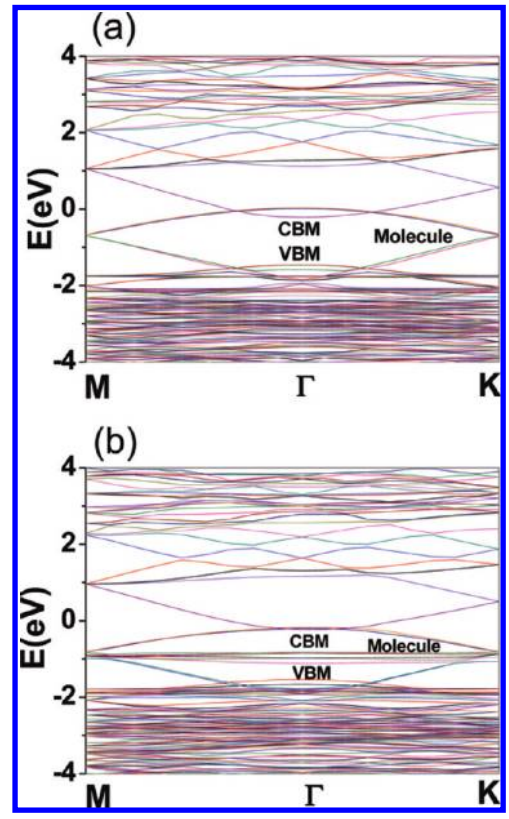

Figure 5. Band structures of full monolayer coverage: (a) monodentate ester-type configuration; (b) bidentate chelating with hydrogen bonding configuration.

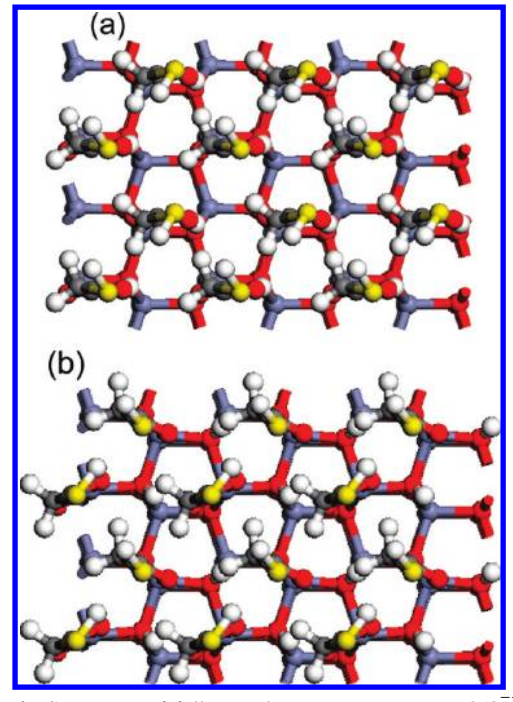

Figure 6. Structures of full monolayer coverage on ZnO(2$\bar{1}\bar{1}$0): (a) top view of monodentate ester-type configuration; (b) top view of bidentate chelating with hydrogen bonding configuration.

also investigated. Both monodentate ester-type and bidentate chelating with hydrogen bonding configurations are involved on this surface. Figure 6 shows the optimized structures of molecular monolayer on ZnO(2$\bar{1}\bar{1}$0). The intermolecular interaction has strong influence on the assembly morphology of molecule. ZnO(2$\bar{1}\bar{1}$0) surface 1 × 1 is used as the substrate.

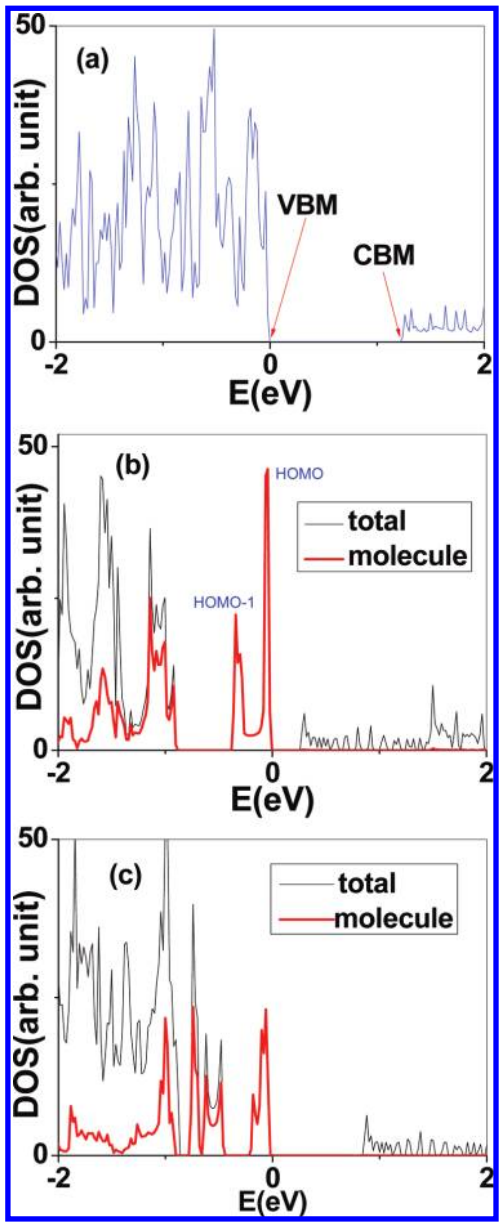

Figure 7. DOS of full monolayer functionalized ZnO($2\bar{1}\bar{1}0$): (a) DOS of clean ZnO($2\bar{1}\bar{1}0$) with 1.22 eV band gap; (b) DOS of monodentate ester-type configuration; (c) DOS of bidentate chelating with hydrogen bonding configuration.

Full monolayer coverage corresponds to 2 molecules per super cell. The molecular monolayer assembly structure is highly different from ZnO($10\bar{1}0$) case. The clean ZnO($2\bar{1}\bar{1}0$) band gap is 1.22 eV, as shown in Figure 7a. Figure 7b shows the DOS of monodentate ester-type configuration. Molecules contribute to the band gap states, but no metal to insulator transition is found. The energy difference between the CBM and the HOMO is around 0.31 eV. The molecule contributed band gap states split into two peaks, HOMO and HOMO-1, corresponding to two-molecule interaction. For bidentate chelating with hydrogen bonding configuration, with the DOS shown in Figure 7c, the energy difference between the CBM and the HOMO is around 0.93 eV. The molecular monolayer contributes an abundance of band gap states into ZnO, but the band gap of ZnO has not been fully filled. The occupied molecular orbitals (below VBM) have strong hybridization with ZnO valence band and tend to be more delocalized. So mercapto-acetic acid molecule functionalized ZnO also shows

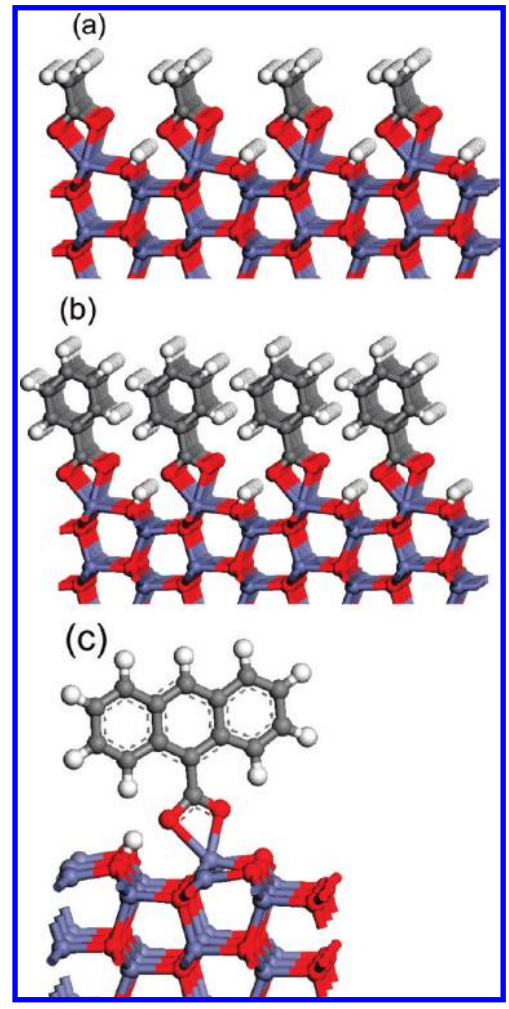

Figure 8. Structure of acetic acid full monolayer, benzoic acid full monolayer, and 9-anthracenecarboxylic acid on surface.

facet dependence and strong configuration dependent electronic structure.

Tail Dependence. The influence of molecular tails on the electronic structure of molecule−semiconductor interface is investigated. The interface between acetic acid, benzoic acid, and 9-anthracenecarboxylic acid on ZnO ($10\bar{1}0$) with configuration (e) are calculated, and the structure optimization results are shown in Figure 8. The DOS is shown in Figure 9.

Figure 9a shows the DOS of isolated acetic acid molecule, and its LUMO−HOMO difference is 5.22 eV. Acetic acid does not contribute to the band gap states of ZnO, as shown in Figure 9b, and is consistent with the self-consistent charge density functional tight binding calculation of carboxylic acid on ZnO($10\bar{1}0$) in ref 18. The LUMO−HOMO difference for benzoic acid is 3.96 eV, as shown in Figure 9c. Benzoic acid contributes an abundance of band gap states, with a width around 0.36 eV as shown in Figure 9d. The energy difference between the HOMO and the CBM is 0.86 eV. So it is expected this interface could have a good conductive and photovoltaic performance. The occupied molecular orbitals (below VBM) have strong hybridization with ZnO valence bands and tend to be more delocalized. 9-Anthracenecarboxylic acid is also used as the tail of the −COOH anchor group, which has been studied experimentally on the TiO_2 surface.[29,30] The LUMO−HOMO gap of 9-anthracenecarboxylic acid is 2.14 eV, as shown in Figure 9e. The open circuit potential is 0.70 eV for 9-anthracenecarboxylic acid from its DOS distribution in Figure 9f, in contrast to the

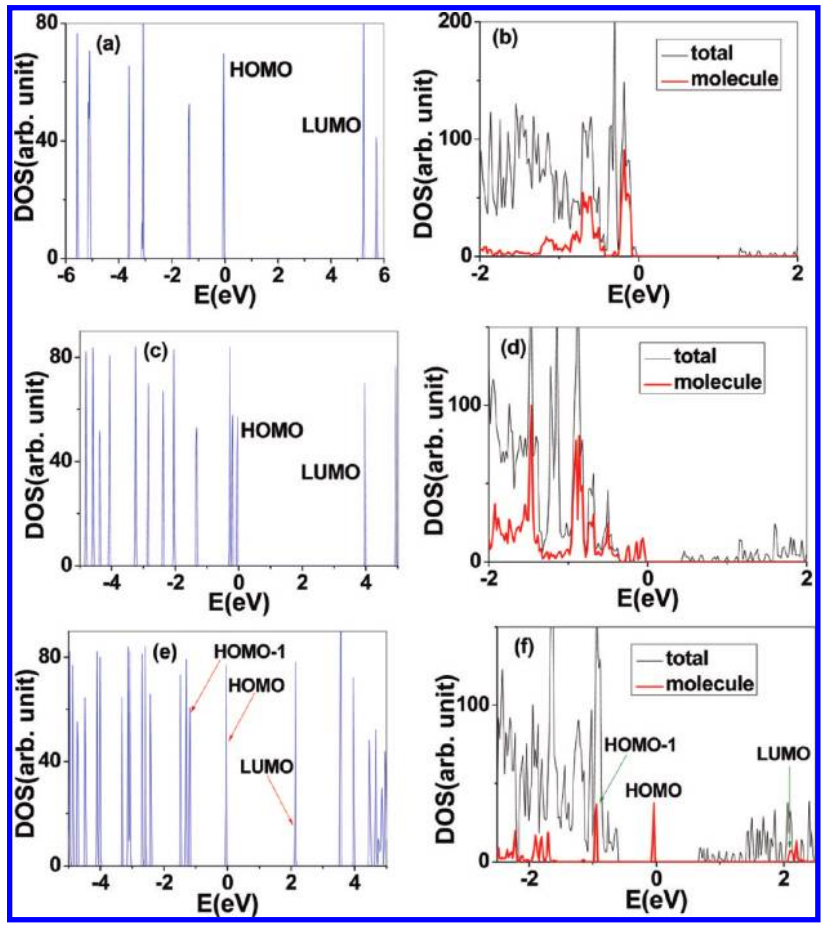

Figure 9. DOS of acetic acid full monolayer, benzoic acid, and 9-anthracenecarboxylic acid on ZnO surface: (a) DOS of isolated acetic acid molecule with 5.22 eV LUMO−HOMO gap. (b) DOS of acetic acid monolayer functionalized surface. (c) DOS of isolated benzoic acid molecule with 3.96 eV LUMO−HOMO gap. (d) DOS of benzoic acid monolayer functionalized surface. (e) DOS of isolated 9-anthracenecarboxylic acid molecule with 2.14 eV LUMO−HOMO gap.(f) DOS of 9-anthracenecarboxylic acid functionalized surface.

same situation for mercapto-acetic acid with 0.86 eV in configuration (e). The occupied molecular orbitals HOMO-1 and below have strong hybridization with ZnO valence band, since there exist peaks at the same energy levels with ZnO.

IV. Conclusion

Mercapto-acetic acid molecule is investigated as the major molecule for carboxylic acid molecules adsorption on ZnO(10$\bar{1}$0). For $^1/_6$ monolayer coverage, the electronic structure of mercapto-acetic acid molecule-ZnO interface shows a strong configuration dependence. Mercapto-acetic acid monolayer functionalized ZnO(10$\bar{1}$0) is on the verge of metal to insulator transition, which is consistent with the experimental findings. Mercapto-acetic acid monolayer functionalized ZnO(2$\bar{1}\bar{1}$0) surface does not show metal to insulator transition. Acetic acid does not contribute to the band gap states of the ZnO(10$\bar{1}$0) surface. However, benzoic acid and 9-anthracenecarboxylic acid can contribute an abundance of band gap states into the ZnO(10$\bar{1}$0) surface, whereas 9-anthracenecarboxylic acid functionalized ZnO(10$\bar{1}$0) surface shows a smaller CBM-HOMO energy difference compared to mercapto-acetic acid in the same situation. These results shed light on understanding of the charge carrier characteristics on organic molecule treated ZnO surfaces and pave the way for future applications of organic molecule treated ZnO surfaces, in solar cells and biosensors, as well as oxide surface engineering and molecular electronics.

Acknowledgment. The technical assistance at the High Performance Computing Facilities of Information Technology Service Center, The Chinese University of Hong Kong, is gratefully acknowledged, particularly, by Mr. Frank Ng and Mr. Stephen Chan. Prof. R. Car and Prof. A. Selloni of Princeton University are gratefully acknowledged for cosupervision and stimulating discussions. Prof. Z. L. Wang of Georgia Institute of Technology is gratefully acknowledged for discussions on the experiments. This work is partially supported by Research Grants Council, under Grant No. CUHK2/CRF/08. X.Q.T. thanks CNOOC Grants for financial support during his visit to Princeton University.

References and Notes

(1) (a) Lucas, M.; Mai, W. J.; Yang, R. S.; Wang, Z. L.; Riedo, E. *Nano Lett.* **2007**, *7*, 1314–1317. (b) Wang, X. D.; Zhou, J.; Song, J. H.; Liu, J.; Xu, N. S.; Wang, Z. L. *Nano Lett.* **2006**, *6*, 2768–2772.

(2) (a) Marana, N. L.; Longo, V. M.; Longo, E.; Martins, J. B. L.; Sambrano, J. R. *J. Phys. Chem. A* **2008**, *112*, 8958–8963. (b) Diebolda, U.; Koplitzb, L. V.; Dulub, O. *Appl. Surf. Sci.* **2004**, *237*, 336–342. (c) Meyer, B.; Marx, D. *Phys. Rev. B* **2003**, *67*, 035403−035413. (d) Kresse, G.; private communication with Diebolda. (e) Wander, A.; Schedin, F.; Steadman, P.; Norris, A.; McGrath, R.; Turner, T. S.; Thornton, G.; Harrison, N. M. *Phys. Rev. Lett.* **2001**, *86*, 3811–3814. (f) Wander, A.; Harrison, N. M. *Surf. Sci.* **2000**, *457*, L342–L346.

(3) Matsui, H.; Hasuike, N.; Harima, H.; Tabata1, H. *J. Appl. Phys.* **2008**, *104*, 094309.

(4) Kanai, Y.; Selloni, A. *J. Am. Chem. Soc.* **2006**, *128*, 3892–3893.

(5) Deutsch, D.; Natan, A.; Shapira, Y.; Kronik, L. *J. Am. Chem. Soc.* **2007**, *129*, 2989–2997.

(6) Quintanaa, M.; Marinadob, T.; Nonomurab, K.; Boschloob, G.; Hagfeldt, A. *J. Photochem. Photobiol. A* **2009**, *202*, 159–163.

(7) Lao, C. S.; Li, Y.; Wong, C. P.; Wang, Z. L. *Nano Lett.* **2007**, *7*, 1323–1328.

(8) Kresse, G.; Furthmü ller, J. *Comput. Mater. Sci.* **1996**, *6*, 15–50.

(9) Perdew, J. P.; Chevary, J. A.; Vosko, S. H.; Jackson, K. A.; Pederson, M. R.; Singh, D. J.; Fiolhais, C. *Phys. Rev. B* **1992**, *46*, 6671–6687.
(10) Perdew, J. P.; Wang, Y. *Phys. Rev. B* **1992**, *45*, 13244–13249.
(11) Kresse, G.; Joubert, D. *Phys. Rev. B* **1999**, *59*, 1758–1775.
(12) Dudarev, S. L.; Botton, G. A.; Savrasov, S. Y.; Humphreys, C. J.; Sutton, A. P. *Phys. Rev. B* **1998**, *57*, 1505.
(13) (a) Janotti, A.; Walle, C. G. V. D. *Phys. Rev. B* **2007**, *75*, 121201–121204. (b) Lany, S.; Zunger, A. *Phys. Rev. B* **2008**, *78*, 235104–235128. (c) Kim, Y. S.; Park, C. H. *Phys. Rev. Lett.* **2009**, *102*, 086403–086406. (d) Janotti, A.; Segev, D.; Walle, C. G. V. D. *Phys. Rev. B* **2006**, *74*, 045202–045210.
(14) Wang, J.; Li, Q.; Egerton, R. F. *Micron* **2007**, *38*, 346–353.
(15) Anderson, P. W. *Phys. Rev.* **1961**, *124*, 41–53.
(16) Newnst, M. *Phys. Rev.* **1969**, *178*, 1123–1145.
(17) Gong, X. Q.; Selloni, A.; Vittadini, A. *J. Phys. Chem. B* **2006**, *110*, 2804–2811.
(18) Moreira, N. H.; Rosa, A. L. D.; Frauenheim, T. *Appl. Phy. Lett.* **2009**, *94*, 193109–193111.
(19) Persson, P.; Lunell, S.; Ojamäe, L. *Int. J. Quantum Chem.* **2002**, *89*, 172–180.
(20) Persson, P.; Ojaḿ ae, L. *Chem. Phys. Lett.* **2000**, *321*, 302–308.
(21) Taratula, O.; Galoppini, E.; Wang, D.; Chu, D.; Zhang, Z.; Chen, H.; Saraf, G.; Lu, Y. *J. Phys. Chem. B* **2006**, *110*, 6506–6515.
(22) Tanner, R. E.; Sasahara, A.; Liang, Y.; Altman, E. I.; Onishi, H. *J. Phys. Chem. B* **2002**, *106*, 8211–8222.
(23) Persson, P.; Bergstrm, R.; Lunell, S. *J. Phys. Chem. B* **2000**, *104*, 10348–10351.
(24) Meng, S.; Ren, J.; Kaxiras, E. *Nano Lett.* **2008**, *8*, 3266–3276.
(25) Li, S. C.; Wang, J. G.; Jacobson, P.; Gong, X. Q.; Selloni, A.; Diebold, U. *J. Am. Chem. Soc.* **2009**, *131*, 980–984.
(26) Angelis, F. D.; Fantacci, S.; Selloni, A.; Gra1tzel, M.; Nazeeruddin, M. K. *Nano. Lett.* **2007**, *7*, 3189–3195.
(27) Wang, Y.; Meyer, B.; Yin, X.; Kunat, M.; Langenberg, D.; Traeger, F.; Birkner, A.; Wo̧ll, Ch. *Phys. Rev. Lett.* **2005**, *95*, 266104–266107.
(28) Deryckei, V.; Soukiassian, P. G.; Amy, F.; Chabal, Y. J.; Angeol, M. D. D.; Enriquezi, H. B.; Silly, M. G. *Nat. Mater.* **2003**, *2*, 253–258.
(29) Kamat, P. V. *J. Phys. Chem.* **1989**, *93*, 859–864.
(30) He, J. J.; Zhao, J. C.; Shen, T.; Hidaka, H.; Serpone, N. *J. Phys. Chem. B* **1997**, *101*, 9027–9034.

JP908517J